Research Article

Yanjun Lu*, Yuxuan Ma, Tong Yang, and Jifeng Guo

Hydrophilic modification of PVDF membranes by *in situ* synthesis of nano-Ag with nano-ZrO_2

https://doi.org/10.1515/gps-2021-0050
received May 19, 2021; accepted July 09, 2021

Abstract: Modified polyvinylidene fluoride (PVDF) membranes were prepared by the phase inversion method via blending *in situ* formed nanosilver (Ag) and nanozirconium dioxide (ZrO_2). Scanning electron microscopy of the membranes revealed that the surface pore size of the membranes was increased and distributed widely with the addition of modified nanosilver (Ag) and nanozirconium dioxide (ZrO_2). The pores of the membrane were reduced due to excessive modification of the material when the content of zirconium dioxide was increased to 0.4%. XRD characterization showed that *in situ* synthesis of nanosilver (Ag) and nanozirconium dioxide (ZrO_2) had been successfully blended in the membranes. The contact angle of the modified membrane ranged from 82.72° to 67.37°, which showed that the hydrophilic properties of the membrane were improved. The pure water flux of the modified membrane increased from 28.43 to 143.2 L/m^2 h, indicating that the hydrophilicity of the modified membrane was enhanced significantly. The flux recovery rate of the modified membrane was obviously increased in the fouling experiment with BSA as the source of organic pollutants. The antimicrobial contamination of the membrane was greatly enhanced with the *E. coli* microbial contamination experiment.

Keywords: hydrophilic modification, PVDF membrane, *in situ* synthesis, Ag with zirconium dioxide nanoparticles, antifouling

1 Introduction

Membrane separation technology, e.g., microfiltration [1,2], ultrafiltration [3,4], nanofiltration [5,6], and reverse osmosis [7,8] plays an important role in the sewage treatment technology, which has wide applications in many fields such as the industrial production separation [9,10], water and wastewater treatment [11], etc. Polyvinylidene fluoride (PVDF), a kind of organic polymer membrane material with the advantages of strong chemical stability, thermal stability, and high mechanical properties, has been used in membrane separation technology. However, the pristine PVDF membrane has strong hydrophobicity, which causes the adhered organic substance to form membrane contamination and then decreases its functionality. Membrane modification is an effective method to resist membrane fouling. The main methods of the hydrophilic modification of PVDF membrane are copolymerization modification and blending modification. Copolymerization is modified by chemical methods to endow the molecular chains of PVDF with hydrophilic groups or monomers to improve the hydrophilicity of the membrane. Zhang polymerized poly(acrylic acid) (PAA) side chains on the PVDF membrane with TiO_2 by sol–gel preparation and found that the hydrophilicity and the antifouling abilities of the membrane were enhanced significantly [11]. PVDF was also blended with the hydrophilic material to improve the hydrophilicity of the membrane [12–18] with a simple and easy blending modification method. The main blending materials are hydrophilic polymers such as PMMA (poly(*N*-isopropyl-acrylamide)) [19], CA (cellulose acetate) [20], PU (polyurethane) [21], etc., or inorganic nanoscale particles such as silica [22], titanium dioxide [23], blending silver [24], alumina [4], etc. It can be found that via blending inorganic nanomaterials, not only the hydrophilic properties and the anti-pollution performances of the membrane can be improved, but the mechanical properties can also be enhanced. Pang modified the PVDF membrane with *in situ* formed nano-ZrO_2 [25], and found that the hydrophilicity and the antifouling performances of the modified PVDF membrane were improved.

---

* **Corresponding author: Yanjun Lu,** School of Civil and Architecture Engineering, Xi'an Technological University, Xi'an 710021, China, e-mail: 191121733@qq.com, tel: +86-02986173264, fax: +86-02986173264
Yuxuan Ma, Tong Yang, Jifeng Guo: School of Water and Environment, Key Laboratory of Subsurface Hydrology and Ecology in Arid Areas, Ministry of Education, Chang'an University, Xi'an 710054, China

In addition, ZrO_2 had higher stability and was suitable for liquid-phase separation under extreme conditions. So, the anti-pollution performance of the anti-organic membrane could be improved by hydrophilic modification [26–29].

Biological fouling is a vital factor induced by the reduction of the membrane flux. Li employed *in situ* formed nanoscale Ag particles to modify the PVDF membrane and found that Ag played an important role in the antimicrobial properties and also could improve the hydrophilic properties of the membrane [30]. However, using Ag as a hydrophilic substance to improve the hydrophilic properties of the PVDF membrane was expensive. So, a cheaper and high efficiency method was developed by the modification of the membrane with two kinds of nanomaterials.

In this paper, a certain amount of $AgNO_3$ as a raw material was used to synthesize nanoscale silver to improve the antimicrobial properties of the membrane, while ZrO_2 as the main material was used to improve hydrophilic properties. The modified PVDF membrane was prepared by the phase inversion method via blending *in situ* formed nanosilver (Ag) and nano-zirconium dioxide (ZrO_2) under ultrasonic dispersion. The membrane was further characterized by XRD and scanning electron microscopy (SEM). Hydrophilic and antifouling performances were also studied to obtain more insights into the membrane properties.

2 Experimental

2.1 Materials

Poly(vinylidene fluoride) (PVDF: CAS: 24937-79-9, FR904, Shanghai) was purchased from Sanaifu. Silver nitrate ($AgNO_3$; analytical grade), and *N,N*-dimethylformamide (DMF; CAS: 68-12-2, $d > 99\%$, reagent) were obtained from Jinhuada Co. Ltd of Guangzhou City; polyvinylpyrrolidone (PVP, CAS: 9003-39-8, reagent) was purchased from Zhengzhoupaini Co., Ltd; nano-zirconium dioxide (ZrO_2) (CAS: 53801-45-9, 50 nm, Shanghai) was obtained from Macklin Biochemical Co., Ltd; and bovine serum albumin (BSA, CAS: 9048-46-8) protein was obtained from Biofroxx.

2.2 Preparation of the Ag/ZrO_2-PVDF membrane

For the preparation of the Ag/ZrO_2-PVDF membrane, $AgNO_3$ (0.5%) was dissolved in an appropriate amount of DMF stirring until the solution changed from light yellow to brown and then nano-ZrO_2 particles were added and dispersed ultrasonically for 30 min in a 50°C water bath. In another container, PVP (1%) was dissolved in DMF, and then PVDF (15%) was continuously added. The mixture was stirred in a water bath at 50°C to obtain a homogeneous clear solution. The Ag/ZrO_2 solution was added into a uniform PVDF solution and stirred for 3 h at 50°C in a water bath to obtain a yellow casting solution, indicating that a well-dispersed Ag and ZrO_2 solution was obtained, which was then dispersed ultrasonically for 30 min and allowed to stand one day for removing the bubbles and to obtain a homogeneous casting solution. The casting solution was poured into a glass plate that was washed with ethanol and deionized water, and then the membrane was scraped with a scratch knife until the plate was naturally dried. The glass was then put in deionized water to induce the liquid-liquid phase conversion to obtain the membrane PVDF and Ag/ZrO_2-PVDF 0–4. PVDF membrane is a pristine membrane, Ag/ZrO_2-PVDF 0–4 is a nanosized silver and nanoscale-zirconia modified membrane, where 0–4 refer to the modified membrane prepared under different concentrations of zirconium dioxide (Table 1).

2.3 Characterization of the Ag/ZrO_2-PVDF membrane

X-ray diffractometer (XRD, Bruker AXS Co., Ltd., D8 ADVANCE) was used to analyze the surface compositions of the membranes with a copper Kα radiation source at a scan rate ranging from 10° to 90° at 2°/min. The chemical composition of the membrane was studied using Fourier transform infrared spectroscopy (FTIR-ATR, PerkinElmer Spectrum Two). After drying and spraying the membrane with gold, the surface morphology of the membrane was observed with an SEM (SEM, Hitachi S-4800). The contact

Table 1: Composition of the cast solution (mass%)

	PVDF	Ag/ ZrO_2-PVDF0	Ag/ ZrO_2-PVDF1	Ag/ ZrO_2-PVDF2	Ag/ ZrO_2-PVDF3	Ag/ ZrO_2-PVDF4
PVDF (%)	15	15	15	15	15	15
DMF (%)	84	83.5	83.4	83.3	83.2	83.1
PVP (%)	1	1	1	1	1	1
$AgNO_3$ (%)	0	0.5	0.5	0.5	0.5	0.5
ZrO_2 (%)	0	0	0.1	0.2	0.3	0.4

angle was measured with a contact angle measuring instrument (Shanghai Zhongchen Digital Technology Equipment Co., Ltd., JC2000C). To measure the hydrophilicity of the membrane, 3 µL of water was dropped on the surface of the membrane, and the contact angle meter was used to record for 1 min. Each membrane was tested five times and the averaged data was obtained.

2.4 Flux experiment

The membrane flux and rejection were measured with a flux testing device under 0.1 MPa pressure and at room temperature. First, the membrane was cut into a disc of size 12.56 cm^2 and pre-pressured with deionized water for 30 min to get a stable flux, J_w. BSA rejection was measured at 0.1 MPa and prepressured with deionized water for 30 min; the water flux was recorded every 5 min. The deionized water was replaced by a BSA solution until the flux reached a stable value. The concentration of a certain period of penetration solution is calculated as the rejection R:

$$J_\mathrm{w} = \frac{V}{A \times t} \tag{1}$$

where J_w is the pure water flux of the membrane (L/m^2 h); V is the volume of penetrative water (L); A is the effective membrane area (m^2); and t is the running time (h).

$$R = \left(1 - \frac{C_\mathrm{p}}{C_\mathrm{f}}\right) \times 100\% \tag{2}$$

where R is the rejection of BSA (%); C_P is the concentration of BSA in the permeation solution; and C_f is the concentration of BSA in the feed solution.

2.5 Evaluation of antifouling properties

The multicycle filtration test was used to evaluate the antifouling properties of the membrane. First, the membrane was pre-pressured with deionized water for 30 min at 0.1 MPa and room temperature. The water flux J_W was recorded, the deionized water was replaced by BSA solution, and the flux J_p of the BSA solution was recorded by suction filtration at 0.1 MPa for 30 min. The water flux of the membrane was tested again after the membrane was rinsed with deionized water (J_r). According to the multicycle filtration test, the membrane relative flux reduction and flux recovery ratio were calculated by the following equations:

$$\mathrm{RFR}\ (\%) = \left(1 - \frac{J_\mathrm{p}}{J_\mathrm{w}}\right) \times 100\% \tag{3}$$

$$\mathrm{FFR}\ (\%) = \frac{J_\mathrm{r}}{J_\mathrm{w}} \times 100\% \tag{4}$$

2.6 Evaluation of antibacterial properties

The antibacterial properties of the membrane were evaluated by the inhibition zone method, and the size of the zone of inhibition was a direct indication of the ability to assess the antimicrobial contamination of the membrane. First, the Luria-Bertani (LB) broth in a certain ratio was processed in an autoclave. *E. coli* was inoculated into the liquid LB broth, which was incubated at 37°C for 24 h. Then, the LB agar was sterilized in a certain ratio in an autoclave and poured into a plate. Then, the cultured *E. coli* was inoculated into a solid medium and uniformly coated; then the membrane was cut into a disc of 12.56 cm^2 and placed in a medium inoculated with *E. coli* cultivated for 24 h in an incubator at 37°C and the experiment result was recorded.

3 Results and discussion

3.1 Chemical constitution of the membrane surface

The XRD pattern of the modified PVDF membrane is shown in Figure 1. It can be seen that the diffraction peaks of PVDF appeared in the spectra 1–6 at 2θ around

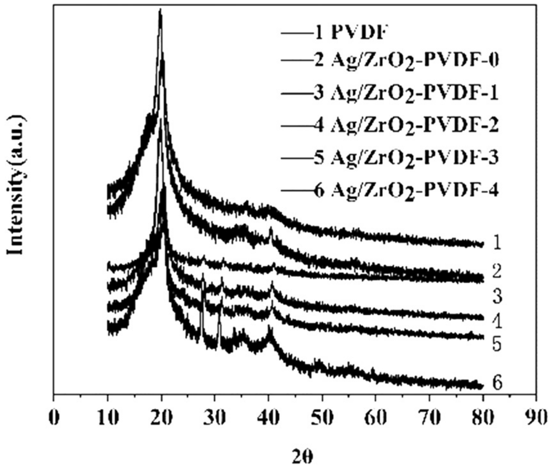

Figure 1: XRD patterns of PVDF, Ag/ZrO$_2$-PVDF-0, Ag/ZrO$_2$-PVDF-1, Ag/ZrO$_2$-PVDF-2, Ag/ZrO$_2$-PVDF-3, and Ag/ZrO$_2$-PVDF-4.

20°, and the intensity of the diffraction peak weakened with the addition of the modified nanosilver and nano-ZrO_2 in the membrane. For the 2–6 XRD pattern, a weak diffraction peak appeared around 2θ of 41°, corresponding to the diffraction peak of nano-Ag. The diffraction peaks of ZrO_2 appeared at 27° and 30° at 2θ in spectra 3–6, corresponding to the monoclinic phases (111) and (−111), respectively. As the concentration of zirconia increased, the peak intensity increased. All the above results demonstrated that nanosilver and nanozirconia are successfully doped into PVDF membranes.

As shown in Figure 2, 1–6 were the Fourier transform infrared spectra (FTIR-ATR) of PVDF, Ag/ZrO_2-PVDF-0, Ag/ZrO_2-PVDF-1, Ag/ZrO_2-PVDF-2, Ag/ZrO_2-PVDF-3, and Ag/ZrO_2-PVDF-4, respectively. In the infrared spectrum of a pristine PVDF membrane, the absorption peak of C–C is at 879/cm, the deformation vibration absorption peak of $-CH_2$ connected to $-CF_2$ is at 1405.6/cm and the stretching vibration absorption peak of CF_2 in PVDF is at 1173.1/cm; and the peak appearing at 1,667/cm corresponds to C═O, which is probably the chemical bond of DMF remaining in the film. The difference from the pristine PVDF spectrum is that the corresponding peak of Zr–O appears at 748.1/cm. The integrated XRD results show that it is ZrO_2, and the intensity of the peak increases with the increase of the content of doped ZrO_2.

3.2 Membrane morphology

Scanning electron micrographs of the PVDF membrane and the modified membrane Ag/ZrO_2-PVDF 0–4 to determine the surface morphology are shown in Figure 3. It can be seen that there are a few pores on the surface of the pristine PVDF membrane, which has a smaller pore size than the modified Ag/ZrO_2-PVDF membrane. On increasing the concentration of ZrO_2, the number of pores increased. When the mass of ZrO_2 was increased to 0.4%, it could be seen that the number of pores was reduced due to the excessive amount of the modified material. The reason for a distinct difference between the pristine membrane and modified membrane was that the stronger repulsive force of PVDF and hydrophilic substance led to the shrinkage of the organic phase in the process of membrane modification. Meanwhile, the addition of hydrophilic materials accelerated the phase separation of the solvent and nonsolvent, resulting in the formation of porous structures. The casting solution became viscous; the speed of phase separation decreased as the content of ZrO_2 increased, and when the content of ZrO_2 increased to 0.4%, the membrane pores agglomerated, which resulted in the decrease in the number of the membrane pores, as shown in Figure 3f.

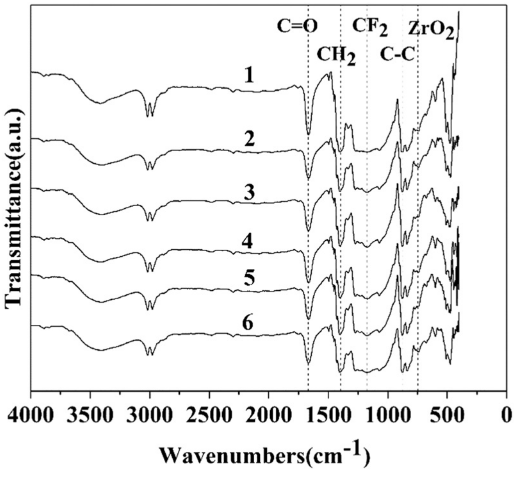

Figure 2: FTIR-ATR spectra of PVDF, Ag/ZrO_2-PVDF-0, Ag/ZrO_2-PVDF-1, Ag/ZrO_2-PVDF-2, Ag/ZrO_2-PVDF-3, and Ag/ZrO_2-PVDF-4.

3.3 Membrane hydrophilicity

The contact angles of the PVDF membrane and Ag/ZrO_2-PVDF membrane are shown in Figure 4. We evaluated the hydrophilicity of the membranes by comparing the contact angles. As shown, the contact angle decreased from 82.72° to 60.13° with the addition of the hydrophilic nanoscale Ag and the amount of nanoscale ZrO_2, thereby increasing the hydrophilicity of the modified membrane. The contact angle of the Ag/ZrO_2 PVDF membrane increased as the mass of ZrO_2 reached 0.4%, possibly due to the agglomeration of ZrO_2 on the membrane surface, which led to the increased roughness of the membrane surface thus increasing the contact angle. The contact angle of the membrane depends on the hydrophilicity of the membrane: the higher the hydrophilicity, the smaller the contact angle. At the same time, the roughness of the membrane surface also has a greater influence on the contact angle. From SEM characterization, it was evident that with the increase of the Ag/ZrO_2, the pore size of the modified PVDF membrane increased. But when the amount of Ag/ZrO_2 reached 1%, the pore size became smaller, and the water flux of the membrane tends to decrease thereby causing an increase in the retention rate. All of the above proved that the hydrophilic properties of the modified Ag/ZrO_2-PVDF membrane increased with the increase of hydrophilic substances. The number of modified substances reached the breaking point when the content of Ag/ZrO_2 is increased to 1%. The surface

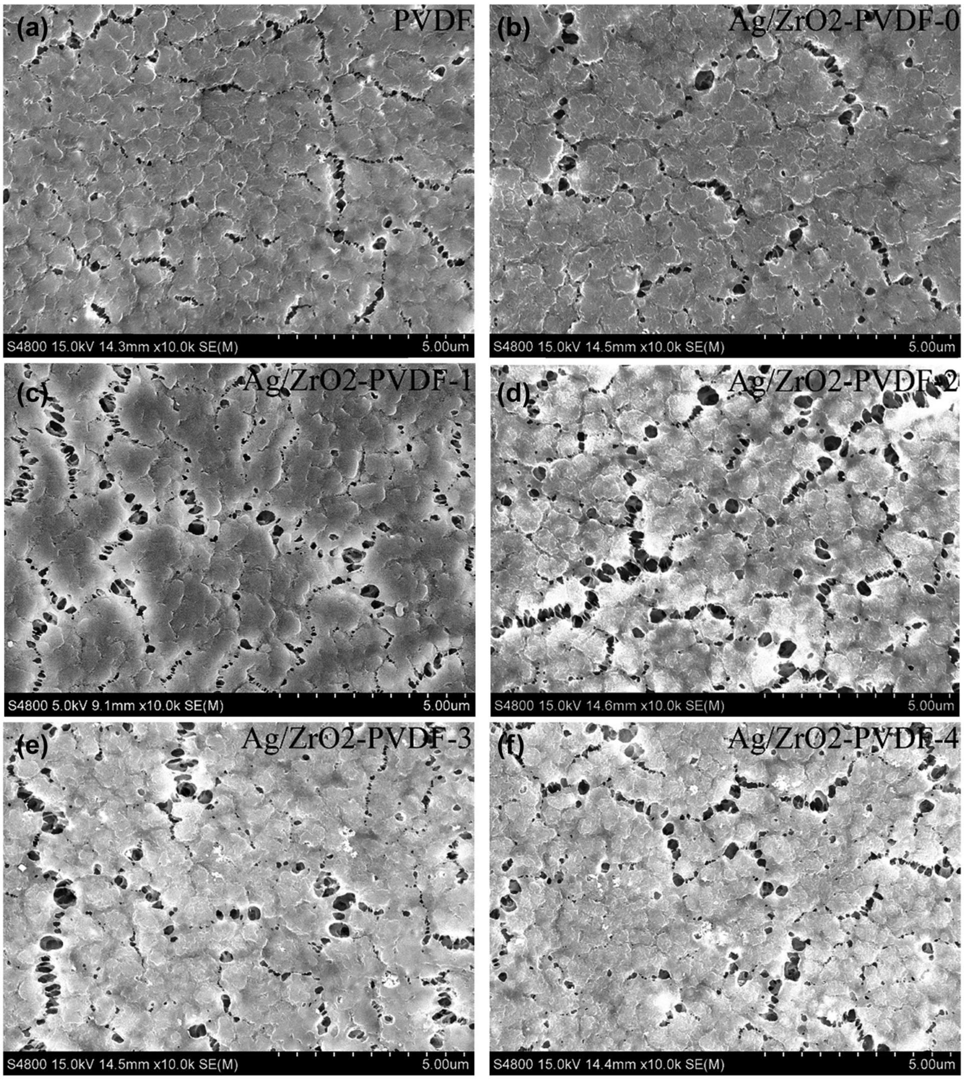

Figure 3: SEM images of membranes to determine the surface morphology: (a) PVDF, (b) Ag/ZrO_2-PVDF-0, (c) Ag/ZrO_2-PVDF-1, (d) Ag/ZrO_2-PVDF-2, (e) Ag/ZrO_2-PVDF-3, and (f) Ag/ZrO_2-PVDF-4.

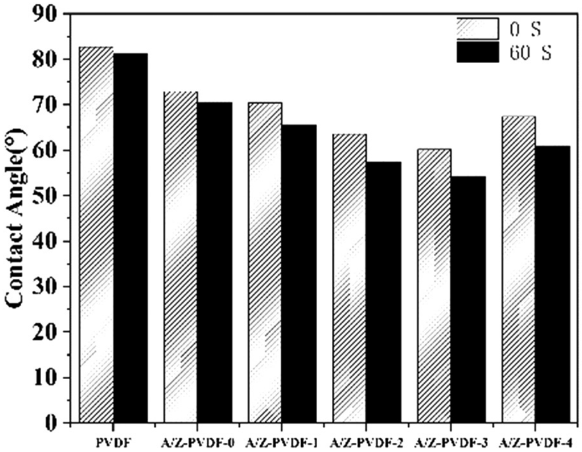

Figure 4: Contact angles of PVDF, Ag/ZrO_2-PVDF-0, Ag/ZrO_2-PVDF-1, Ag/ZrO_2-PVDF-2, Ag/ZrO_2-PVDF-3, and Ag/ZrO_2-PVDF-4.

roughness of the subsequent PVDF membrane increases, which causes an increase in the contact angle.

The changes in the contact angle of the PVDF membrane and the Ag/ZrO_2-PVDF membranes were recorded in this experiment after dropping the water onto the membrane for 1 min. It revealed that the contact angle of the membrane decreased as the hydrophilic substance increased, indicating that the membrane hydrophilicity increases as the amount of hydrophilic material blend increases.

3.4 Filtration performance of the membrane

The water flux and the BSA rejection rate are shown in Figure 5. It can be seen that the water flux of the pristine

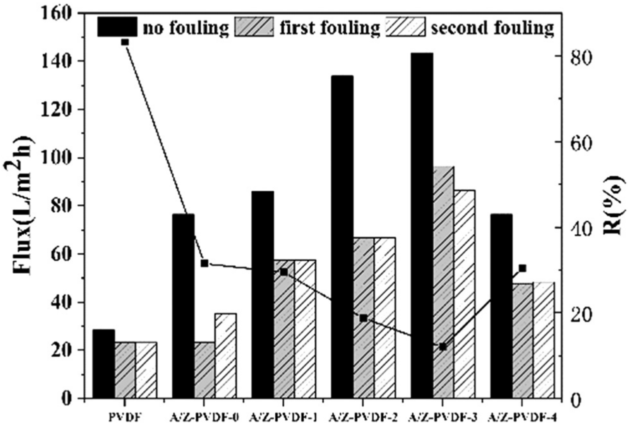

Figure 5: Water flux and BSA rejection rates of PVDF, Ag/ZrO_2-PVDF-0, Ag/ZrO_2-PVDF-1, Ag/ZrO_2-PVDF-2, Ag/ZrO_2-PVDF-3, and Ag/ZrO_2-PVDF-4.

membrane was lower (28.43 L/m^2 h) compared with the modified membrane, which had obviously improved water flux. From SEM characterization, it was evident that with the increase of modified materials, the pore size and distribution of the membrane became larger and wider. The obvious difference between the pure PVDF membrane and Ag/ZrO_2-PVDF membrane was due to the strong repulsion between the PVDF and hydrophilic materials, which led to the shrinkage of the organic phase in the process of membrane modification. At the same time, the addition of hydrophilic materials accelerated the phase separation of the solvent and nonsolvent, resulting in the formation of porous structures. In addition, the increase of the hydrophilic material had a great influence on the water flux. Therefore, the water flux of the pure PVDF membrane is much lower than that of the modified PVDF membrane.

It was found that the membrane water flux decreased significantly after the membrane was contaminated by BSA, which was treated as organic pollutants in the experiment, and then the water flux of the membranes tends to be stable after the recycle contamination experiment. However, the water flux of the membrane tends to decrease when the content of ZrO_2 was increased to 0.4%, which may be contributing to the change in the morphology of the membrane; due to the excessive amount, the blockage of the membrane pore made the water transport difficult. The PVDF membrane had the largest rejection among the membranes, and the reason for the change in the rejection rate of the membrane was due to the addition of the hydrophilic substance, which increased the pore diameter and decreased the adsorption of organic substances such as proteins, etc. However, the rejection rate increased when the ZrO_2 was increased to 0.4%, which was consistent with the reason for the decrease in water flux. Above all, it is evident that the water flux could be increased by modifying the PVDF membrane to improve the hydrophilicity of the membrane.

3.5 Organic antifouling performance of the membrane

The pure water and BSA flux changes of the PVDF membrane and Ag/ZrO_2-PVDF membrane are shown in Figure 6. After the membrane was contaminated with BSA, it was found that the water flux of the membrane dropped significantly, which indicated that BSA caused the membrane surface fouling and inner fouling. The membrane water flux recovers but does not return to the flux level prior to fouling after rinsing with deionized water. A further cycle of membrane fouling experiments revealed that the membrane water flux tended to be stable, which showed that BSA adsorption and diffusion to the surface of the membrane reached equilibrium. The relative flux reduction and flux recovery rate of the PVDF membrane and Ag/ZrO_2-PVDF membrane were obtained through the calculation of two pollution cycle experiments. As shown in Figure 7, the pristine PVDF membrane had the highest RFR and the lowest FRR, which may be due to the strong hydrophobicity of the PVDF membrane and thus irreversible membrane fouling. Figure 7 shows that the flux decay rate of PVDF membranes decreased from 78% of pure PVDF membranes to 65% of Ag/ZrO_2-PVDF (0.5%) membranes. This implies that the modified PVDF membrane in the BSA cyclic

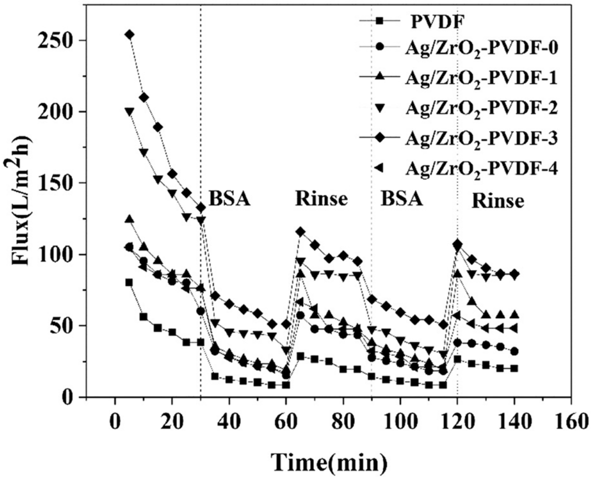

Figure 6: The changes in pure water and BSA flux of PVDF, Ag/ZrO_2-PVDF-0, Ag/ZrO_2-PVDF-1, Ag/ZrO_2-PVDF-2, Ag/ZrO_2-PVDF-3, and Ag/ZrO_2-PVDF-4 with time.

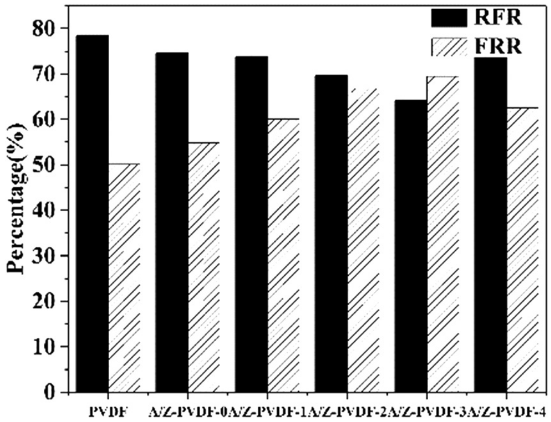

Figure 7: RFR and FRR values of PVDF, Ag/ZrO_2-PVDF-0, Ag/ZrO_2-PVDF-1, Ag/ZrO_2-PVDF-2, Ag/ZrO_2-PVDF-3, and Ag/ZrO_2-PVDF-4 with time.

pollution experiment showed good resistance to protein pollution. The flux recovery rate also increased from 50% of pure PVDF membrane to about 70% of Ag/ZrO_2-PVDF (0.5%) membrane, indicating that the modified membrane had better anti-pollution performance compared with the pure PVDF membrane. The strong hydrophobicity of the PVDF membrane can easily cause the blockage and fouling of BSA in the pores severely, and thus lead to irreversible membrane fouling. As the content of hydrophilic substances increased, a hydration layer was formed on the membrane surface, the relative flux of the membrane decreased, and the flux recovery rate increased. So, the hydrophilic modification can protect the membrane from organic pollution effectively.

Hydrophilic modification of the membrane revealed a decrease in the relative flux reduction of the membrane flux and an increase in the rate of flux recovery, indicating that the membrane can be more effectively protected against organic pollution by hydrophilic modification.

3.6 Bacterial antifouling performance of the membrane

In this experiment, the inhibition zone method was used to evaluate the antibacterial properties of the membrane.

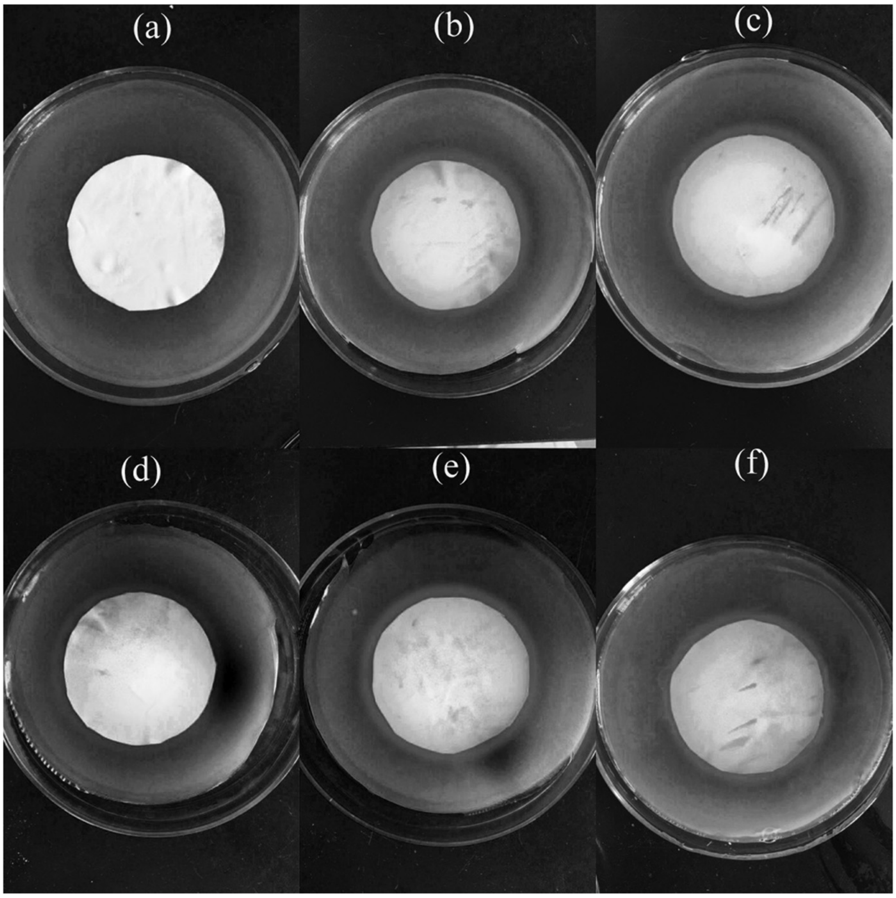

Figure 8: The effect of Ag on the inhibition zone thickness of (a) PVDF, (b) Ag/ZrO_2-PVDF-0, (c) Ag/ZrO_2-PVDF-1, (d) Ag/ZrO_2-PVDF-2, (e) Ag/ZrO_2-PVDF-3, and (f) Ag/ZrO_2-PVDF-4 with time.

As shown in Figure 8, the PVDF membrane was contaminated during the cultivation of *E. coli* in Figure 8a, which illustrated that the pure PVDF membrane had no inhibitory effect on *E. coli*. It was clear that the zone of inhibition is formed around the PVDF membrane modified by *in situ* nanosilver blending in Figure 8b, which counteracted microbial contamination effectively. Meanwhile, the size of the suppression band formed in Figure 8c–f was almost the same as in Figure 8b, thus illustrating that the modification of the PVDF membrane by blending nanoscale-silver ions synthesized by *in situ* synthesis method was an effective method for protection from contamination by the antimicrobial.

4 Conclusion

In this experiment, the PVDF membrane was modified with nanoscale-zirconia and *in situ* synthesis of nanoscale-silver by the phase inversion method and blending modification.

It was found that the number and the size of pores were increased first and then decreased with the increase of hydrophilic materials, and the contact angle decreased by 15.35° with the increase of the content of hydrophilic polymer and the water flux significantly improved. This indicated that the surface morphology of the PVDF membrane was affected by the formed blending nanoscale-Ag and nanoscale-ZrO_2, thus making a significant improvement in the hydrophilic properties of the membrane. After the membrane was contaminated with BSA as an organic pollutant, it revealed that the flux recovery of the membrane increased with the increase of hydrophilicity, indicating that the anti-fouling performance of the Ag/ZrO_2-PVDF membrane after modification was improved. At the same time, the pristine PVDF membrane and Ag/ZrO_2-PVDF membrane contaminated by *E. coli* indicated that the nanoscale-silver ions synthesized by the *in situ* synthesis method have a significant effect on the microbial antifouling performance of the membrane. In conclusion, the properties of the modified Ag/ZrO_2-PVDF film have been greatly improved.

Funding information: This research was supported by the Natural Science Foundation of Shaanxi Province, China (2019JQ-838).

Author contributions: Yanjun Lu: writing – original draft, writing – review and editing, conceptualization, methodology, formal analysis, data curation, supervision, funding acquisition; Yuxuan Ma: writing – review and editing, resources, investigation; Tong Yang: resources, investigation, visualization; Jifeng Guo: writing – review and editing.

Conflict of interest: The authors state no conflict of interest.

Data availability statement: The datasets generated and analyzed during the current study are available from the corresponding author on reasonable request.

References

[1] Wang X, Wang Z, Chen H, Wu Z. Removal of Cu(II) ions from contaminated waters using a conducting microfiltration membrane. J Hazard Mater. 2017;339:182–90. doi: 10.1016/j.jhazmat.2017.06.038.

[2] Zhu L, Chen M, Dong Y, Tang CY, Huang A, Li L. A low-cost mullite-titania composite ceramic hollow fiber microfiltration membrane for highly efficient separation of oil-in-water emulsion. Water Res. 2016;90:277–85. doi: 10.1016/j.watres.2015.12.035.

[3] Bae TH, Tak TM. Effect of TiO_2 nanoparticles on fouling mitigation of ultrafiltration membranes for activated sludge filtration. J Membr Sci. 2005;249(1):1–8. doi: 10.1016/j.memsci.2004.09.008.

[4] Lu Y, Yu SL, Chai BX, Xianda S. Effect of nano-sized Al_2O_3-particle addition on PVDF ultrafiltration membrane performance. J Membr Sci. 2006;276(1):162–7. doi: 10.1016/j.memsci.2005.09.044.

[5] Cheng XQ, Shao L, Lau CH. High flux polyethylene glycol based nanofiltration membranes for water environmental remediation. J Membr Sci. 2015;476:95–104.doi: 10.1016/j.memsci.2014.11.020.

[6] Harisha RS, Hosamani KM, Keri RS, Nataraj SK, Aminabhavi TM. Arsenic removal from drinking water using thin film composite nanofiltration membrane. Desalination. 2010;252(1):75–80. doi: 10.1016/j.desal.2009.10.022.

[7] Cadott JE, Petersen RJ, Larson RE, Erickson EE. A new thin-film composite seawater reverse osmosis membrane. Desalination. 1980;32(1–3):25–31. doi: 10.1016/S0011-9164(00)86003-8.

[8] Konagaya S, Kuzumoto H, Watanabe O. New reverse osmosis membrane materials with higher resistance to chlorine. J Appl Polym Sci. 2000;75(11):1357–64. doi: 10.1002/(SICI)1097-4628(20000314)75:11<1357:AID-APP6>3.0.CO;2-W.

[9] Ghazali AA, Abd Rahman S, Abu Samah R. Potential of adsorbents from agricultural wastes as alternative fillers in mixed matrix membrane for gas separation: a review. Green Process Synth. 2020;9(1):219–29. doi: 10.1515/gps-2020-0023.

[10] Marino T, Blefari S, Di Nicolo E, Figoli A. A more sustainable membrane preparation using triethyl phosphate as solvent. Green Process Synth. 2017;S16(3):295–300. doi: 10.1515/gps-2016-0165.

[11] Zhang F, Zhang W, Yu Y, Deng B, Li J, Jin J. Sol–gel preparation of PAA-g-PVDF/TiO_2 nanocomposite hollow fiber membranes

with extremely high water flux and improved antifouling property. J Membr Sci. 2013;432(7):25–32. doi: 10.1016/j.memsci.2012.12.041.

[12] Rana D, Matsuura T, Narbaitz RM, Feng C. Development and characterization of novel hydrophilic surface modifying macromolecule for polymeric membranes. J Membr Sci. 2005;249(1–2):103–12. doi: org/10.1016/j.memsci.2004.09.034.

[13] Rana D, Matsuura T, Narbaitz RM. Novel hydrophilic surface modifying macromolecules for polymeric membranes: polyurethane ends capped by hydroxy group. J Membr Sci. 2006;282(1–2):205–16. doi: 10.1016/j.memsci.2006.05.024.

[14] Kim Y, Rana D, Matsuura T, Wook-Jin C. Influence of surface modifying macromolecules on the surface properties of poly (ether sulfone) ultra-filtration membranes. J Membr Sci. 2009;338(1–2):84–91. doi: 10.1016/j.memsci.2009.04.017.

[15] Kim Y, Rana D, Matsuura T, Chung WJ, Khulbe KC. Relationship between surface structure and separation performance of poly (ether sulfone) ultra-filtration membranes blended with surface modifying macromolecules. Sep Purif Tech. 2010;72(2):123–32.doi: 10.1016/j.seppur.2010.01.006.

[16] Rana D, Kim Y, Matsuura T, Arafat HA. Development of antifouling thin-film-composite membranes for seawater desalination. J Membr Sci. 2011;367(1–2):110–8. doi: 10.1016/j.memsci.2010.10.050.

[17] Rana D, Scheier B, Narbaitz RM, Matsuura T, Tabe S, Jasim SY, et al. Comparison of cellulose acetate (CA) membrane and novel CA membranes containing surface modifying macromolecules to remove pharmaceutical and personal care product micropollutants from drinking water. J Membr Sci. 2012;409–410:346–54. doi: 10.1016/j.memsci.2012.04.005.

[18] Rana D, Narbaitz RM, Garand-Sheridan AM, Westgate A, Matsuura T, Tabe S, et al. Development of novel charged surface modifying macromolecule blended PES membranes to remove EDCs and PPCPs from drinking water sources. J Mater Chem A. 2014;2(26):10059–72. doi: 10.1039/c4ta01530d[17].

[19] Ochoa NA, Masuelli M, Marchese J. Effect of hydrophilicity on fouling of an emulsified oil wastewater with PVDF/PMMA membranes. J Membr Sci. 2003;226(1):203–11. doi: 10.1016/j.memsci.2003.09.004.

[20] Razzaghi MH, Safekordi A, Tavakolmoghadm M, Rekabdar F, Hemmati M. Morphological and separation performance study of PVDF/CA blend membranes. J Membr Sci. 2014;470:547–57. doi: 10.1016/j.memsci.2014.07.026.

[21] Lü X, Wang X, Guo L, Zhang Q, Guo X, Li L. Preparation of PU modified PVDF antifouling membrane and its hydrophilic performance. J Membr Sci. 2016;520:933–40. doi: 10.1016/j.memsci.2016.08.018.

[22] Wu H, Mansouri J, Chen V. Silica nanoparticles as carriers of antifouling ligands for PVDF ultrafiltration membranes. J Membr Sci. 2013;433(15):135–51. doi: 10.1016/j.memsci.2013.01.029.

[23] Rahimpour A, Jahanshahi M, Rajaeian B, Rahimnejad M. TiO_2, entrapped nano-composite PVDF/SPES membranes: preparation, characterization, antifouling and antibacterial properties. Desalination. 2011;278(1):343–53. doi: 10.1016/j.desal.2011.05.049.

[24] Kim Y, Rana D, Matsuura T, Chung WJ. Towards antibiofouling ultrafiltration membranes by blending silver containing surface modifying macromolecules. Chem Commun. 2012;48(5):693–5. doi: 10.1039/c1cc16217a.

[25] Pang RZ, Li X, Li JS, Lu ZY, Huang C, Sun XY. In situ preparation and antifouling performance of ZrO_2/PVDF hybrid membrane. Acta Physico-Chimica Sin Acta Phys-Chim Sin. 2013;29(12):2592–8(7). doi: 10.3866/PKU.WHXB201310291.

[26] Kaur D, Bagga V, Behera N, Thakral B, Asija A, Kaur J, et al. SnSe/SnO_2 nanocomposites: novel material for photocatalytic degradation of industrial waste dyes. Adv Compos Hybrid Mater. 2019;2(4):763–76. doi: 10.1007/s42114-019-00130-7.

[27] Zhao YY, Zhang YQ, Li FR, Bai YP, Pan YL, Ma J, et al. Ultra-robust superwetting hierarchical membranes constructed by coordination complex networks for oily water treatment. J Membr Sci. 2021;627(1):119234. doi: 10.1016/j.memsci.2021.119234.

[28] Zhang Y, Guo J, Han G, Bai Y, Ge Q, Ma J, et al. Molecularly soldered covalent organic frameworks for ultrafast precision sieving. Sci Adv. 2021;7(3):eabe8706. doi: 10.1126/sciadv.abe8706.

[29] Zhang Y, Cheng X, Jiang X, Urban JJ, Lau CH, Liu S, et al. Robust natural nanocomposites realizing unprecedented ultrafast precise molecular separations. Mater Today. 2020;36:40–7. doi: 10.1016/j.mattod.2020.02.002.

[30] Li X, Pang R, Li J, Sun X, Shen J, Han W. In situ formation of Ag nanoparticles in PVDF ultrafiltration membrane to mitigate organic and bacterial fouling. Desalination. 2013;324(14):48–56. doi: 10.1016/j.desal.2013.05.021.